Appendix

Extension to AETIAQ – Exhaust Plume Measurements at Cranfield

A1. Introduction

A further series of measurements was made at Cranfield in February 2009 with the following objectives:-

1) To acquire a statistically robust dataset of the dispersion of the exhaust jet from the FAAM aircraft under uniform operating conditions.
2) To field test an optical particle counter and analyser (SPARCLE) developed by the University of Oxford (Dr Don Grainger, Dr Dan Peters) against tyre smoke from the FAAM aircraft. (It had originally been intended to field test SPARCLE as part of the main AETIAQ programme, but delays in its development had prevented this.)

The extension trials were programmed for w/c 2 February. This was not a good choice – the runway was under 20 cm of snow! Meteorological conditions eventually permitted us to set up on Monday 16 February and make all our measurements the following day. The delay was of some value in as much as it allowed colleagues from the University of Cambridge (Prof Rod Jones, Dr Iq Mead) to prepare a set of point monitors ("Type A") to be deployed within the aircraft exhaust plume. This appendix reports the measurements taken; inevitably, it can only present a very preliminary analysis.

A2. Experimental Arrangements

The following instruments were available for the study:-

MMU

- The UV Rapid-Scanning Lidar.
- An associated meteorological station (wind speed, direction, temperature and humidity at 10 m; short-wave radiation at 3 m; temperature and humidity at 1.5 m)
- A Doppler Lidar (radial wind speed at a typical height of 100 m)
- 2-off Osiris optical particle counters (PM_{10}, $PM_{2.5}$, PM_1 + wind speed and direction)

Cambridge

- 10-off Type A point monitors (NO, NO_2, CO)

Oxford

- SPARCLE (particle size, number and optical properties)
- Optical particle counter (particle size and number)
- Condensation particle counter (particle number)

FAAM

- Flight data recorder (altitude, Mach no., fuel flows etc.)
- GPS location
- Background O_3 and NO_x.

The overall layout of the instruments is shown in Figure A1. The two Lidars and associated meteorological equipment were collocated on the hard standing beside an airfield service building. (This also provided shelter and power). The Cambridge instruments were deployed under the expected path of the aircraft exhaust plume (4 in the near field; 6 in the far field, all at 10 m separation). The Oxford instruments were deployed in the expected path of the tyre smoke from landing. An Osiris was deployed at each location, as indicated by the 4-pointed stars. These instruments are the height of a man and painted white, so they also served as convenient alignment targets for the Lidar. The Osiris associated with the Type A sensors was located in the centre of the far array in the morning and at the SE end of the near array in the afternoon.

All these point monitors could be deployed manually. The Type A monitors, in particular, were remarkably straightforward to deploy, being lightweight, self-logging and battery-powered. A 0.5 m length of angle iron was driven into the ground at each monitoring point and the monitor lashed to this with cable ties.

It had been planned that the University of Reading (Dr Moira Hilton) should also deploy a scanning mobility particle sizer and a condensation particle counter to monitor aerosol within the exhaust plume. These required vehicular access, however, and since the airfield was basically a swamp at the time (standing water on heavy clay) they could not be used.

The aircraft made eight take-off and landing circuits, with a 10 s burst on full power before each take-off. Four sorties were made in the late morning (from 1000z) and four in the early afternoon (from 1300z). This programme was chosen so that ambient conditions should have changed as little as possible between sorties, and indeed they changed little, with the 10 m wind speed remaining at about 4 m s^{-1} and the direction veering from about 300^o to about 320^o. Conditions were generally bright but overcast – it started to rain as the final sortie was finishing. The aircraft's starting weight was 37 t (the maximum permitted), diminishing by 450 kg on each sortie.

For the first sortie, the aircraft started from ~50 m beyond the piano keys; for all the others, it started from their SW margin. The runway was dry in this area, so there should have been no interference with the Lidar measurements from water spray.

As indicated in Figure A1, an Osiris (with a cup and vane set) was located in the far array of Type A monitors for the morning sorties and in the near array for the afternoon sorties. In either case, it served as the target for the primary scanning azimuth of the Lidar as the aircraft took off. In the case of the morning sorties, however, the Lidar was then swung to the 98.9^o azimuth in the hope of catching the plume as it dispersed further downwind. As the aircraft came in to land, the azimuth was switched to 173.3^o in order to catch the tyre smoke as it advected over the Osiris and SPARCLE.

A3. Observations

Figure A2 shows the wind direction measured by the Osiris and the concentration of NO_x measured with one of the Type A monitors (A17). These were both located at the centre of the far array (cf. Figure A1). It may be seen that the wind vane should provide a convenient set of time-stamps for the take-off and landing of the aircraft. As the aircraft powers up, the wind backs from the ambient 300^o towards the direction of the jet blast, i.e. towards alignment with the runway at 211°. The concentration of NO and NO_2 rise simultaneously, though against a rather noisy background. It is interesting to see that the wind vane also responds to the aircraft's approach: this is presumably from the passage of the wing vortices.

Figure A3 shows an expanded set of NO, NO_2 and CO measurements from the penultimate sortie in the afternoon. Sadly, the Osiris clock (i.e. logging the wind vane) appears to be drifting. We are currently measuring its rate of drift so as to be able to reset the timing of its wind and aerosol measurements. The NO_x peaks are well correlated with the variation of engine load on the flight data recorder. It would appear that we see our maximum CO while the engines are on idle; as they go to full power, CO drops and NOx rises. That said, the CO background does seem to drift. Although the Lidar could detect an elevated plume at the distance of the monitors, it could see nothing at the ground. It would seem, therefore, that the Type A sensors are much more sensitive to the overall mix of exhaust plume constituents at a given point than is the Lidar.

Figures A4 and A5 show the development of the exhaust jet. These broadly show the same dynamics as have been discussed in the main body of the report, but the moderate cross-wind has now permitted us to sample the plume at greater travel times. In its initial phase, the jet forms a head, followed by a ground-hugging plume (a consequence of the Coanda effect). The head eventually leaves the ground as a consequence of the buoyancy of the emission. Both phases may be seen in single frames in these two Figures. The shallow main jet may be seen at ~200 m from the Lidar; as the aircraft starts to move, this is advected laterally away from the Lidar. As the series continue, this plume is seen to advect downwind, gradually dispersing vertically. This section of the plume was seen clearly with the Oxford CPC for all sorties – as was a plume from the aircraft as it taxied up the runway prior to take-off. The head of the jet, meanwhile, is slower and deeper and is advected back across the scanning plane after a travel time of ~14 s. Initially it remains in contact with the ground (Figure A4) but after a further 10-15 s, parts of it may be well clear of the ground (Figure 5). In the morning series, the Lidar was switched from 81.1° to 98.9° after elements of the plume were no longer visible on the real-time monitor. Some traces of plume were then detected at greater distances downwind.

The particular geometry of this field trial thus permitted different elements of the exhaust jet to be sampled at several distances downwind.

Figure A6 then shows a puff of tyre smoke (Sortie 8) in relation to the PM sampling equipment. Out of the eight sorties, tyre smoke was only detected with the Lidar on six of them, most distinctly on Sortie 8: the pilot had been asked to make a deliberately heavy landing on this last flight. Burning rubber or kerosene was smelled by the operators for all landings.

The condensation particle counter detected the aerosol plume from the aircraft in all three modes, taxiing, take-off and landing (Figure A7). Interestingly, the peak number count in the aerosol plume while taxiing was as large as - or greater - than that in the plume on take-off ($3\text{-}8 \times 10^5$ cm^{-3}). Clearly, although the fuel burn while taxiing is only 13% of that in the take-off run, the aircraft is moving an order of magnitude more slowly and there is no airframe lift – reducing both longitudinal and transverse dilution. The particulate number concentration in the tyre smoke on landing was rather smaller ($1\text{-}2 \times 10^5$ cm^{-3}). High concentrations of tyre smoke, however, give a strong signal on the optical particle counters and on the Lidar, since such aerosol is much coarser than that from engine exhausts. It is interesting that the signal on the Lidar was much more time-restricted than that on the nearby CPC: the observed puff had a peak concentration corresponding to about 50% above ambient backscatter and passed though between the scans of 14:15:29 and 14:15:33, the latter scan catching the tail end of it. The peak on the CPC, meanwhile, had a duration of 39 s (full-width, half maximum) starting at about 14:16:00. The Osiris detected nothing at this time beyond the general noise.

Overall, it is clear that, although the Lidar has the capability to monitor aerosol over a broad area, the CPC is a much more sensitive instrument at a single point. We may note that although the Lidar detected tyre smoke on ¾ of landings, this was often at a different range from the location of the point samplers: the implication is that most of the CPC signals on landing in fact arose from the engine emissions, at a concentration below the minimum detection limit for the Lidar. Also, most of the CPC landing plumes were clearly bimodal (cf. Figure A7). This probably reflects the interaction of the wing vortices with the ground.

A4. Discussion

The extension project has thus delivered 8 successful sorties with the FAAM aircraft to add to the 9 which we already had from the main part of the AETIAQ project. The exhaust plume was detected with the Lidar on all take-offs, sometimes at more than one advection distance. With this extension, we have thus more than doubled our stock of plume height statistics. In particular, we have now extended the ranges over which the plume has been sampled to the point at which its buoyant head leaves the ground. Given the uniformity of conditions during the day, we also now have a handle on the variance of plume dispersion under given physical conditions.

More extensive measurements would be very helpful to characterize the nature of the smoke emitted from tyres on landing and the factors which determine the quantity emitted. While the Lidar is flexible in its detection of tyre smoke, point samplers must be directly downwind of the point of touch-down. Many more trials will be needed to acquire a reliable sample.

The CPC measurements have demonstrated that point concentrations from engine emissions on taxiing can be as large as or larger than those from the take-off run. It is also clear that the nature of the tyre smoke on landing is quite different from that of the engine smoke: the latter, being ultra-fine aerosol, is well detected by the CPC and weakly detected by the Lidar; the former must be much coarser since it seems to be practically invisible to the CPC, while it is well detected by the Lidar (or by eye). Despite this, the thermal emission associated with tyre smoke usually allows it to disperse buoyantly over travel distances of a few hundred metres.

The Type A sensors have shown great promise for a first field trip. They clearly have good sensitivity and an adequate time response. They can be deployed rapidly and operated autonomously.

The Osiris, by contrast, was rather disappointing. Aside from the problems with its internal clock, it saw rather little aerosol from the aircraft above the general noise.

We await analysis of the SPARCLE measurements.

Dr Michael Bennett
Centre for Air Transport and the Environment
Manchester Metropolitan University

m.bennett@mmu.ac.uk

3 March 2009

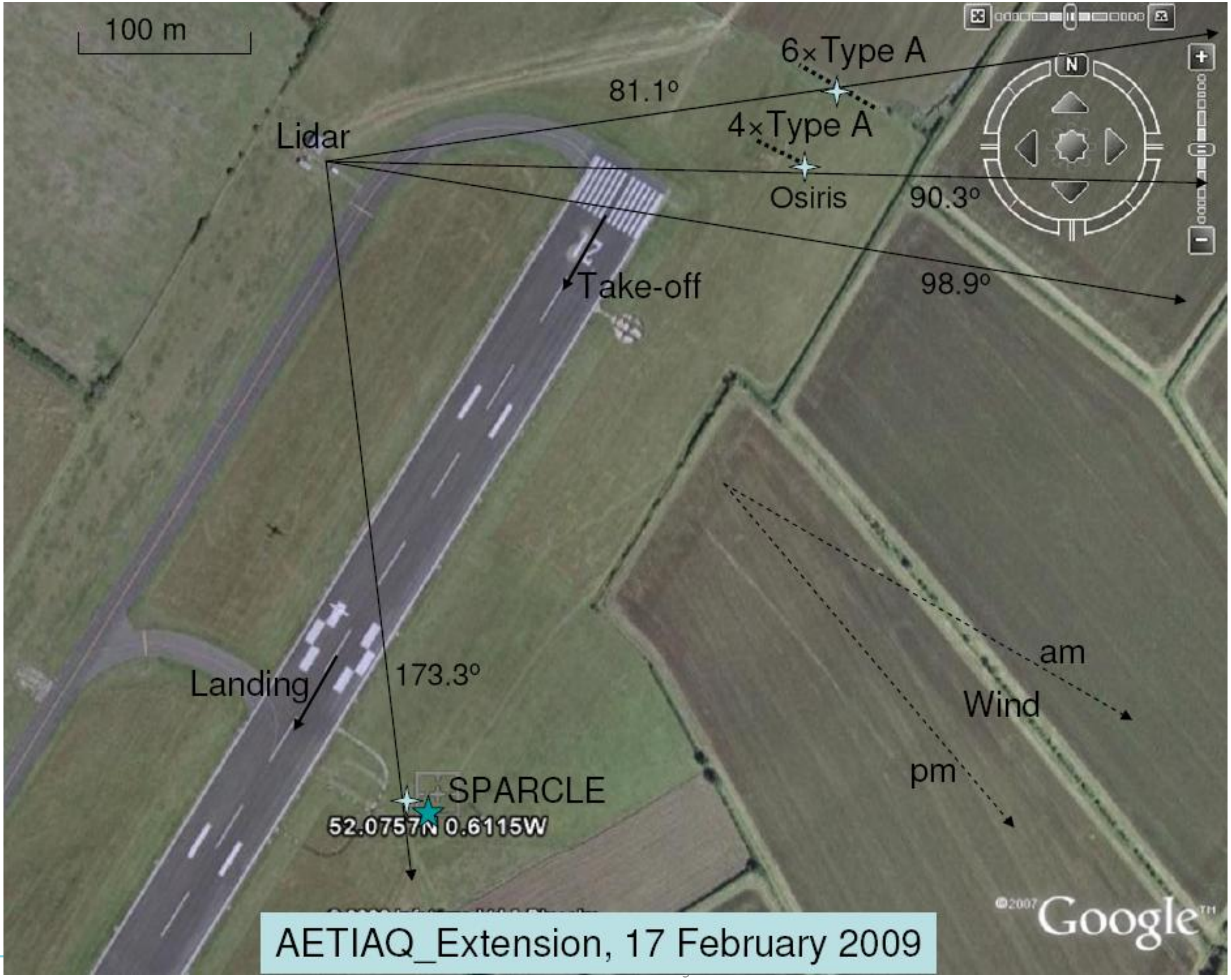

100 m
6×Type A
81.1°
Lidar
4×Type A
Osiris
90.3°
Take-off
98.9°
am
Wind
pm
Landing
173.3°
SPARCLE
52.0757N 0.6115W
AETIAQ_Extension, 17 February 2009
©2007 Google

Figure A1 Layout of instruments for AETIAQ Extension study.

Figure A2 Osiris wind direction and NO_x from Type A monitor in centre of far array, Sorties 1-4.

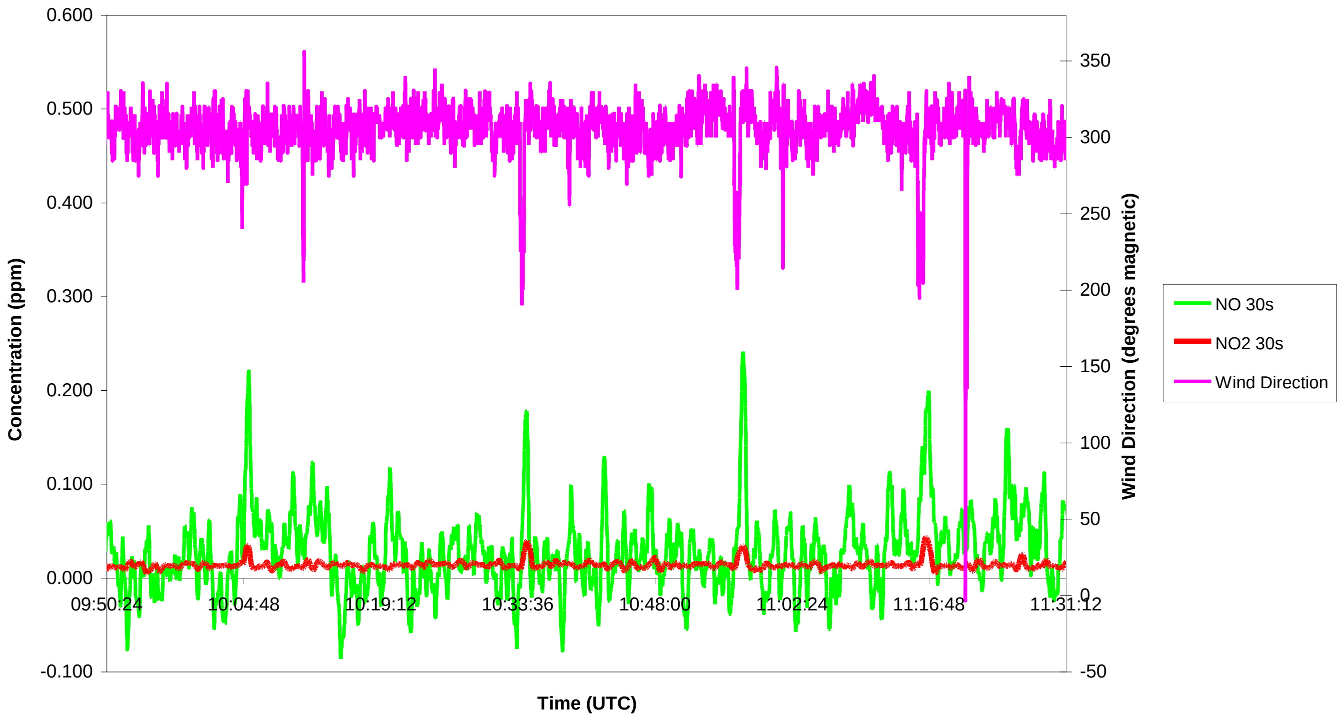

Figure A3 Osiris wind direction and NO_x & CO from Type A monitor in centre of far array, Sortie 7. The third spike of wind direction is from a light aircraft coming in to land.

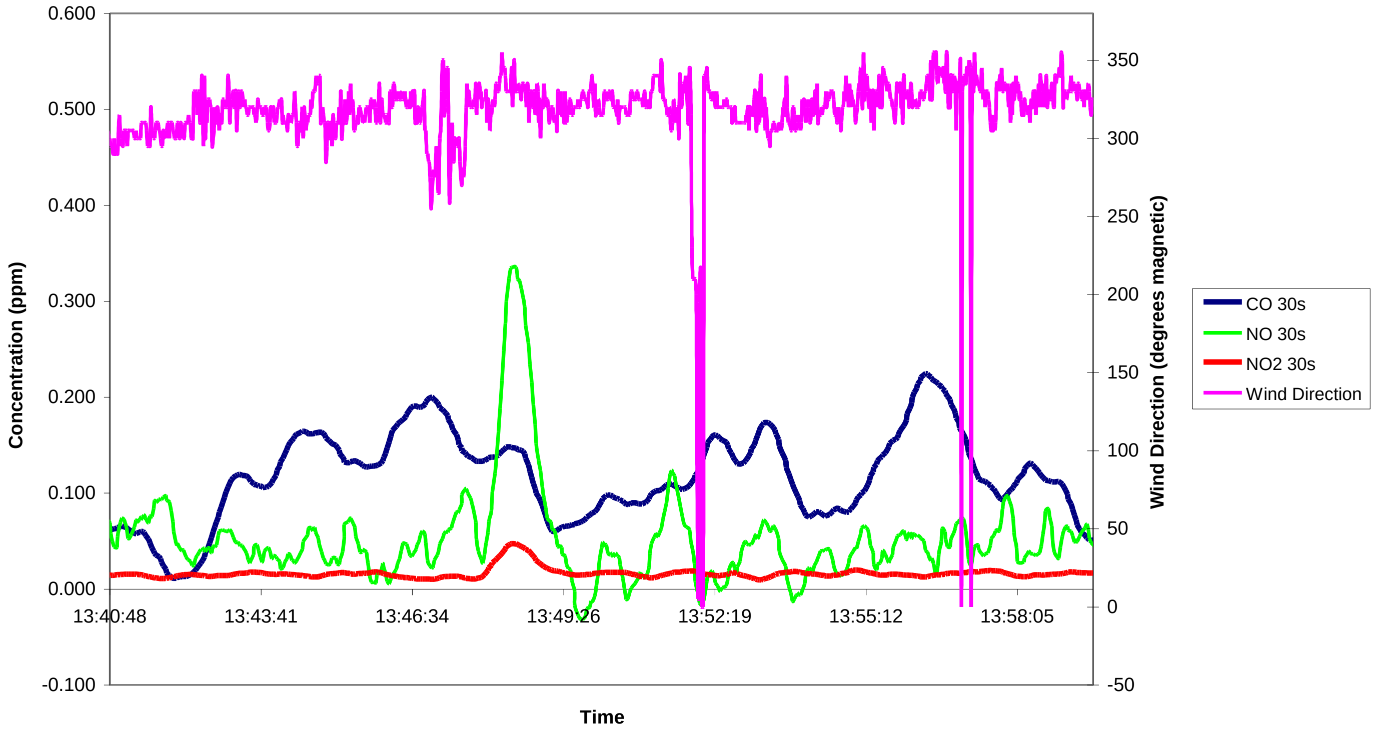

Figure A4 Lidar cross-section of take-off exhaust plume. Time 13:48:14. Azimuth 90.3°. The height datum is the Lidar mirror, which should be about 4 m above the runway surface. The dark shapes below datum are reflections from the ground. The aircraft powered up at about 13:48:00 but was still stationary at the time of the scan. The lowest contour corresponds to an excess backscatter of 4% above ambient, red to an excess of 14%.

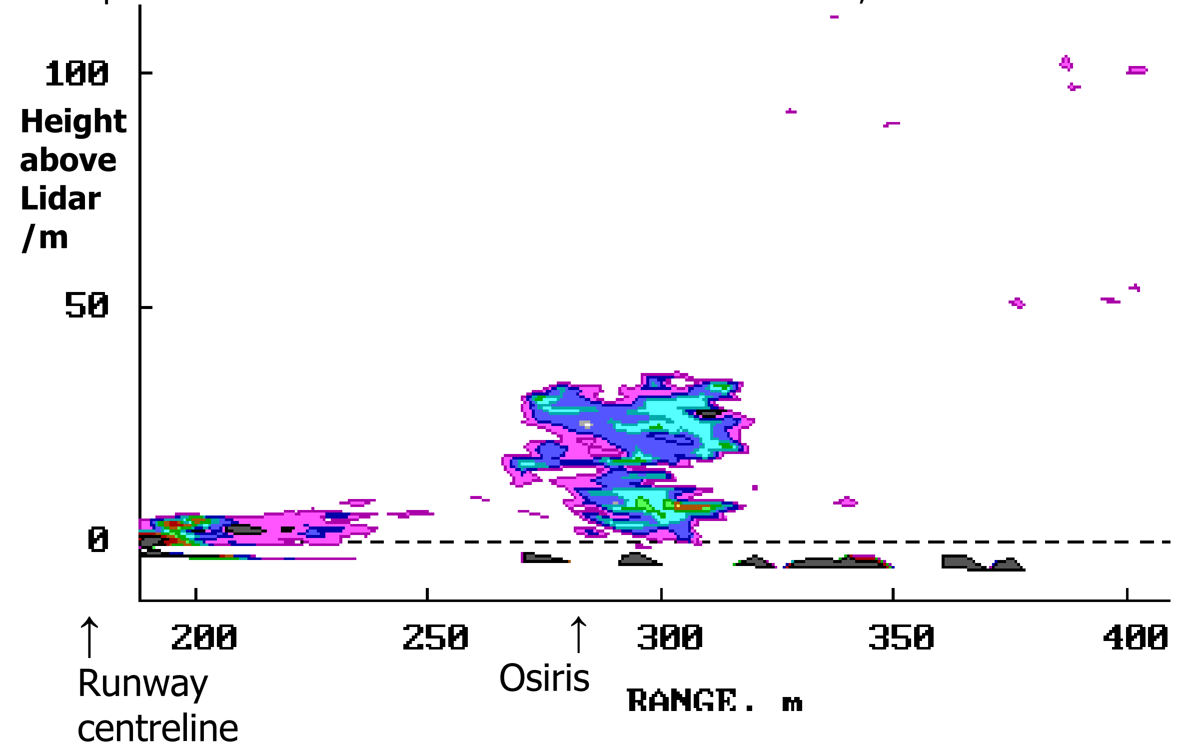

Figure A5 Lidar cross-section of take-off exhaust plume. Time 14:10:53. Azimuth 90.3°. The aircraft powered up at about 14:10:27 and started moving at 14:10:43. The lowest contour corresponds to an excess backscatter of 4% above ambient, black to an excess of 16%.

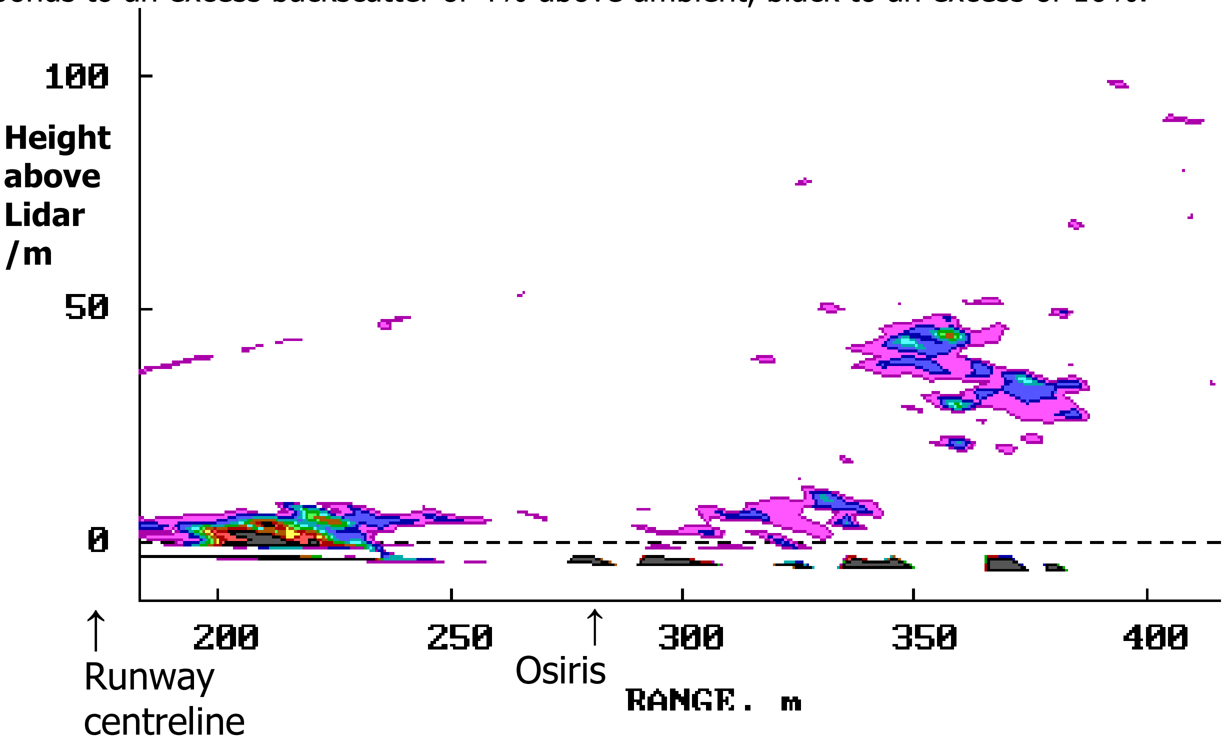

Figure A6 Lidar cross-section of tyre smoke from touch-down at the end of the last sortie. Time 14:15:29. Azimuth 173.3°. The aircraft touched down at 14:15:07. The smoke at this point would have travelled about 60 m from the point of release. The lowest contour corresponds to an excess backscatter of 5% above ambient, black to an excess of 35%.

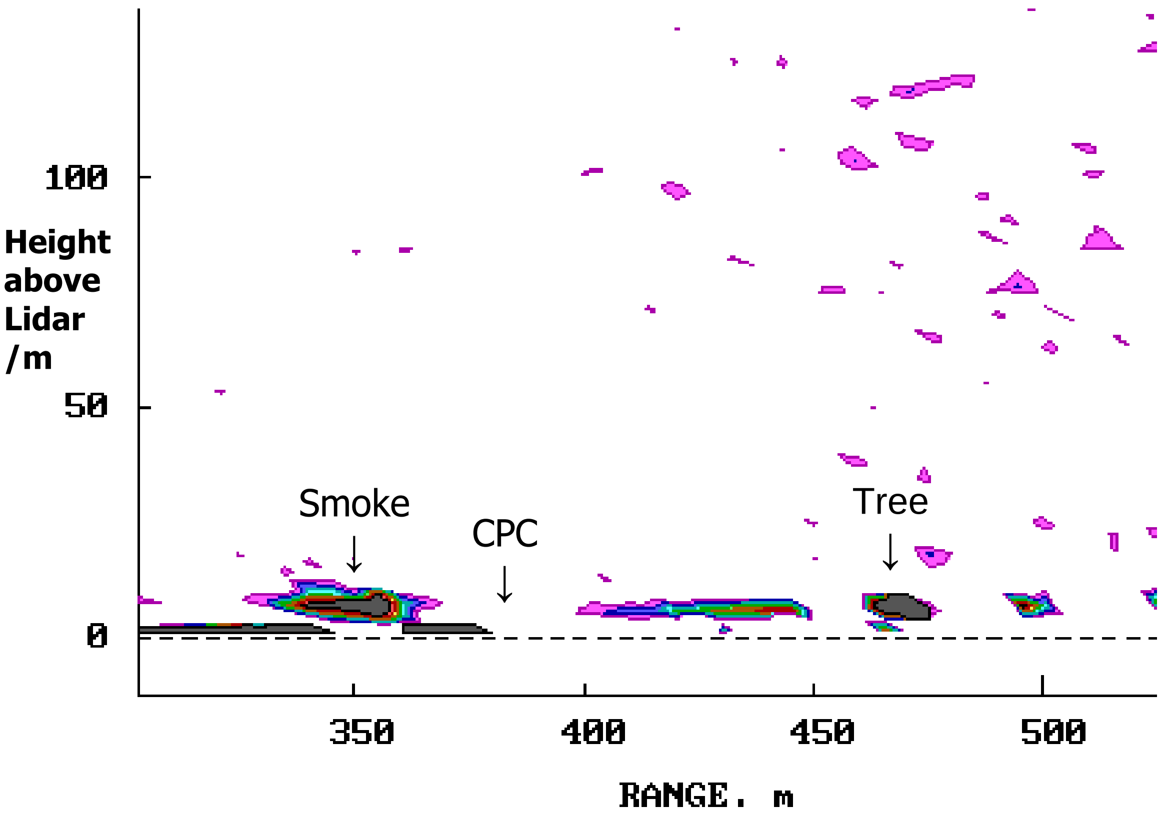

Figure A7 Particle number concentrations for the final sortie from the condensation particle counter (CPC) beside the SPARCLE. These seem to arise almost exclusively from the engine smoke. The first spike is from the aircraft taxiing out; the second from the take-off run; and the third from landing. The Lidar detected a compact puff of tyre smoke which would have passed through the range of the CPC detector at 14:15:32.